Estimation of multiple-quantum well laser parameters for simulation of dispersion supported transmission systems at 20 Gbit/s

M.M. Freire and H.J.A. da Silva

Abstract: In this paper, a set of multiple-quantum well (MQW) laser parameters is proposed for simulation of optical transmission systems at 20 Gbit/s. The parameters have been estimated by joint fitting of a small signal intensity modulation (IM) response model to five measured IM response curves of a strained layer MQW laser, using the Levenberg–Marquardt method. Good agreement between theoretical and experimental curves was obtained. Using these laser parameters, we have assessed the performance of dispersion supported transmission systems at 20 Gbit/s incorporating an erbium doped fibre amplifier (EDFA) or a semiconductor optical amplifier (SOA) as a booster amplifier. It is shown that the use of a SOA, with an unsaturated gain of 20 dB, improves the system performance for link lengths ranging from 8 to 20 km of standard single-mode fibre (SMF) due to partial chirp compensation in the SOA, and degrades the system performance between 1.2 and 2.5 dB for link lengths ranging from 30 to 50 km. The increase of the unsaturated gain of the SOA from 20 to 25 dB is only advantageous for link lengths ranging from 8 to about 12.5 km where a small performance improvement, less than or equal to 0.8 dB, is observed. The influence on the system performance of an increase of the laser line width enhancement factor from 2 to 3 is also investigated.

1 Introduction

Several sets of laser parameters have been published for simulation of optical transmission systems at 10 Gbit/s [1, 2]. Two new methods for extraction of laser parameters have also been reported. In [2], a technique is described for extraction of laser rate equation parameters using measurements of the threshold current and of the output power, resonance frequency and damping factor, at a bias current well above the threshold current. Another new technique is described in [3] for extraction of laser parameters from intermodulation measurements of composite second-order and composite third-order distortion products.

However, with the increase of the bit rate up to 40 Gbit/s in optical transport networks, semiconductor lasers with 3 dB bandwidths of about 20 GHz are required if the four-level dispersion supported transmission (DST) method is used [4, 5]. As far as we know, a set of multiple-quantum well (MQW) laser parameters for simulation of optical transmission systems at 20 Gbit/s has not been published up to now. Due to the lack of a consistent set of laser parameters for simulation of optical transmission systems at 20 Gbit/s, a set of MQW laser parameters is here presented for this purpose. Using this set of laser parameters, we have assessed the performance of 20 Gbit/s dispersion supported transmission systems incorporating an erbium doped fibre amplifier (EDFA) or a semiconductor optical amplifier (SOA) as a booster amplifier. In [6] it was shown that the chirp reduction in a SOA improves, for long link lengths, the performance of optical transmission systems using directly modulated lasers at 4.8 Gbit/s. Here, the use of a SOA is also considered in order to investigate the influence of partial chirp compensation on the performance of DST systems operated at 20 Gbit/s. The use of SOAs may also become attractive due to their low cost, easy fabrication process, yield, reliability and compatibility with standard low cost packaging techniques [7].

2 Estimation of MQW laser parameters

The set of MQW laser parameters has been estimated by joint fitting of an intensity modulation (IM) response model to five measured IM response curves of a strained layer MQW laser consisting of an active layer with eight strained quantum wells of 7 nm thickness and 1% compressive strain, separated by barriers of 8 nm thickness, 0.9% tensile strain and bandgap 1.35 μm. The active layer thickness is 0.056 μm, the active layer width is 1.3 μm, the cavity length is 150 μm, and the confinement factor is 0.114. All details about this laser, which we had access to, have been made available by Working Group 1 of COST 240 in the WWW (world wide web) at the URL given in [8]. More information about COST 240 (techniques for modelling and measuring advanced photonic telecommu-

IEE Proceedings online no. 19990447
DOI: 10.1049/ip-opt:19990447
Paper first received 7th October 1998, and in revised form 19th March 1999

M.M. Freire is with the Department of Mathematics and Computer Science, University of Beira Interior, Rua Marquês d'Ávila e Bolama P-6200, Covilhã, Portugal
E-mail: mfreire@alpha.ubi.pt
H.J. da Silva is with the Department of Electrical Engineering, University of Coimbra–Pole II, Pinhal de Marrocos P-3030, Coimbra, Portugal
E-mail: hjas@ci.uc.pt

nications components) can be found in [9, 10]. The IM response model of MQW lasers was obtained by applying the small signal analysis to the rate equations of MQW lasers given in [11, 12]. Although we have obtained very good fittings for individual curves, the simultaneous fitting of the five curves was very poor. We have then included thermal effects on the IM response model, since some lasers exhibit a strong nonlinear dependence on temperature. A description of the used thermal model follows.

It is well known that long wavelength InGaAsP semiconductor lasers exhibit a strong temperature dependence of the threshold current [13–23]. Several mechanisms have been proposed to explain the observed high temperature sensitivity of the threshold current, such as direct and phonon-assisted Auger recombination processes [15–19], intervalence band absorption [20, 21], a strong temperature dependence of the differential gain [22], and the net optical gain [23]. Other researchers have also suggested that the exponential dependence of the threshold current on temperature, proposed by Pankov in 1968 [24] and widely accepted, is inappropriate [23, 25]. While there is no consensus on temperature dependence, it is generally agreed that Auger recombination is the dominant cause of the dependence of threshold current with temperature [13, 15–19]. Here, we also assume that Auger recombination causes the strong temperature sensitivity of the threshold current and, as a consequence, we consider that, in steady state, the laser mean temperature is proportional to the nonradiative dissipated power. In [26], a thermal model for semiconductor lasers is proposed by Birne and Keating. The temperature dependent parameters considered in their model are the optical gain and the carrier density at transparency. Here, we have considered the carrier lifetime as the temperature dependent parameter instead of the optical gain and the carrier density at transparency, since the threshold carrier density does not increase as rapidly with increasing temperature as does the threshold current [13]. In the model of Byrne and Keating, the laser temperature is dependent on the input current and voltage. Since the laser input power is much larger than the radiated optical power, and the laser mean input voltage is practically constant, we assume here that the laser temperature is proportional to the laser mean input current. Thus, the bimolecular recombination lifetime (carrier lifetime) may be written as [27]:

$$\tau_n = \tau_{n0} e^{-k_T I_b} \tag{1}$$

where τ_{n0} is the bimolecular recombination lifetime at a reference temperature, k_T is a thermal constant dependent on the laser thermal characteristics and I_b is the laser mean input current. The threshold current of MQW lasers also depends on the thermionic emission time from the quantum wells, and it has been shown [12] that this parameter also depends on temperature, but we have ignored this temperature dependence. Despite its simplicity, this model has proved to produce reasonable results, and it has been used to fit theoretical models to measured laser characteristics [28] and in the simulation of optical transmission systems [27].

To perform the joint fitting of the five curves, the χ^2 merit function of the Levenberg–Marquardt method [29] needs to be extended to handle several curves. For an extension to m curves, the merit function may be written as:

$$\chi^2(a) = \sum_{i=1}^{N_1}\left[\frac{R(\omega_i, I_{b1}) - H(\omega_i, I_{b1}, a)}{\sqrt{m}\sigma_i}\right]^2 + \sum_{i=1}^{N_2}\left[\frac{R(\omega_i, I_{b2}) - H(\omega_i, I_{b2}, a)}{\sqrt{m}\sigma_i}\right]^2 + \cdots + \sum_{i=1}^{N_m}\left[\frac{R(\omega_i, I_{bm}) - H(\omega_i, I_{bm}, a)}{\sqrt{m}\sigma_i}\right]^2 \tag{2}$$

where $R(\omega_i, I_{bj})$ (with $j = 1, \ldots, m$) is the measured value of the IM response for the angular frequency ω_i at a bias current I_{bj}, and $H(\omega_i, I_{bj}, a)$ is the theoretical value of the IM response obtained for the angular frequency ω_i at a bias current I_{bj} using the set of laser parameters denoted by a; $N = N_1 + \cdots + N_m$ is the sum of all IM response points obtained for m different bias currents, and σ_i is the standard deviation of the measured values. This method may be applied to joint fitting of several kinds of curves, such as IM response or FM response, since derivatives of $H(\omega_i, I_{bj}, a)$, in order to each parameter of a, are known at ω_i. However, only IM response curves were made available in COST 240; therefore, five IM response curves ($m = 5$) have been fitted for the bias currents of 25, 30, 40, 55, and 70 mA. The total data points of the five IM response curves considered in the fitting was 1670. All values of the five measured IM responses were stored in a vector for the IM response, ordered by increasing bias current, from 25 to 70 mA. The corresponding frequency values of the measured data points at each bias current have been stored in a frequency vector.

For the laser under study, the values of V_w, and Γ (see Table 1 for their meaning) were provided by Working Group 1 of COST 240. As a consequence, we have fixed these two parameters to these constant values and minimised the function given by eqn. 2 with respect to the other laser parameters which may be estimated from IM response measurements. The value of the merit function (least squares residual) for the optimal set of parameters is 82.2, which reveals a good fitting of the modelled curves to the measured ones, as shown in Fig. 1. It is not possible to estimate all laser parameters from IM response measurements. Thus, typical values for the parameters which were not estimated (V_s, g_b, α, η) are also listed in Table 1. The values considered for g_b and η have been reported in [27],

Table 1: MQW laser parameters for simulation at 20 Gbit/s

Parameter description	Value
Volume of the quantum wells (V_w)	$10.92\,\mu m^3$
Volume of the SCH (V_s)	$43.68\,\mu m^3$
Optical confinement factor (Γ)	0.114
Spontaneous emission factor (β_{sp})	2.4403×10^{-4}
Differential gain in the wells (g_0)	4.9643×10^{-12} m^3/s
Parameter of the SCH (g_b)	4.17×10^{-13} m^3/s
Carrier density at transparency (N_0)	1.2859×10^{24} m^{-3}
Bimolecular recombination lifetime at a Reference temperature (τ_{n0})	0.6898 ns
Transport time across the SCH (τ_{cap})	5.7374 ps
Thermionic emission time out (τ_{esc})	231.4 ps
Photon lifetime (τ_p)	0.4954 ps
Gain compression factor (ε)	3.5450×10^{-23} m^3
Line width enhancement factor (α)	2
Differential quantum efficiency (η)	0.0442 W/A
Thermal constant (k_T)	15.8372 A^{-1}
Emission wavelength (λ_0)	1550 nm

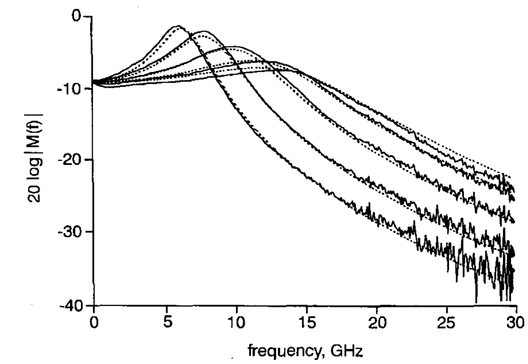

Fig. 1 *Measured and modelled curves of IM response at 25, 30, 40, 55 and 70 mA*

and V_s is assumed to be four times higher than V_w [27]. The value of 2 was taken for the line width enhancement factor (α), since this is a typical value for a strained layer MQW laser with eight quantum wells [30]. The estimated laser parameters listed in Table 1 are typical, with the exception of the value of the spontaneous emission factor (β_{sp}) which is slightly higher. A better way to estimate this parameter is from RIN (relative intensity noise) measurements, but these were not available. This parameter is very important since it was shown [31] that the contribution due to frequency-to-intensity conversion of laser phase noise, after propagation *via* dispersive fibres, is responsible for the BER floor observed in DST experiments at 10 Gbit/s for distances around 253 km SMF [32]. However, at 20 Gbit/s the maximum link length is less than 80 km (see Section 4), and no BER floors (close to 10^{-9}) have been observed in our simulations even with this slightly higher value of β_{sp}.

3 Modelling and simulation methodology

In this Section, we describe the methodology used for simulation and performance assessment of dispersion supported transmission systems. The block diagram of the simulated DST system at 20 Gbit/s is shown in Fig. 2, and a brief description of the system model follows. The pseudo pattern generator (PPG) provides a pseudo random binary sequence (PRBS) with 2^7-1 bits. The optical transmitter includes a laser driver and a MQW laser. Assuming the laser driver behaves as a nonideal current source, the NRZ drive current applied to the laser is generated with exponential rising and falling edges. The rise and fall times (between 20 and 80%) of the pulses are assumed to be 10.6 and 10.8 ps, respectively. For simulation of the dynamic response of MQW lasers, a rate equation model given in [11, 12] has been used jointly with a rate equation for the phase of the emitted optical field [28]. This model describes the carrier dynamics in quantum wells and in the separate confinement heterostructure (SCH), and the photon dynamics in the laser cavity, yielding the following set of equations written in terms of volumetric densities:

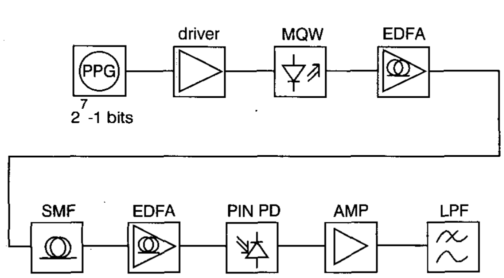

Fig. 2 *Block diagram of simulated 20 Gbit/s DST system*

$$\frac{dN_b}{dt} = \frac{I}{qV_w} - \frac{N_b}{\tau_{cap}} - \frac{N_b}{\tau_n} + \frac{N_w}{\tau_{esc}} \tag{3}$$

$$\frac{dN_w}{dt} = \frac{N_b}{\tau_{cap}} - \frac{N_w}{\tau_{esc}} - \frac{N_w}{\tau_n} - g_0\frac{N_w - N_0}{1+\varepsilon S}S \tag{4}$$

$$\frac{dS}{dt} = \Gamma g_0 \frac{N_w - N_0}{1+\varepsilon S}S - \frac{S}{\tau_p} + \Gamma\beta_{sp}\frac{N_w}{\tau_n} \tag{5}$$

$$\frac{d\phi}{dt} = \frac{\alpha}{2}\Gamma g_0(N_w - N_{wr}) + (1-\Gamma)g_b\frac{V_w}{V_s}(N_b - N_{br}) \tag{6}$$

with

$$N_b = N_s\frac{V_s}{V_w} \tag{7}$$

where N_b is a fictitious density, N_s is the carrier density in the SCH, N_w is the carrier density in the quantum wells, S is the photon density in the laser cavity, ϕ is the phase of the optical field, I is the injection current, q is the electronic charge, N_{wr} is the carrier density in the quantum wells for the reference bias level, N_{br} is the fictitious density corresponding to the carrier density in the SCH for the reference bias level, and the other symbols are defined in Table 1.

Erbium-doped fibre amplifiers (EDFAs) are assumed to be used in the configurations of booster and preamplifier and they have been modelled as wide-band linear repeaters. The EDFA used as optical preamplifier is assumed to have an equivalent noise bandwidth of 1 THz and a noise figure of 6 dB [33, 34]. The use of a SOA as a booster amplifier, instead of an EDFA, is also considered in order to investigate the influence of partial chirp compensation, due to self-phase modulation in the SOA, on the performance of DST systems. Using the approximation in which the internal loss is much smaller than the gain, the SOA may be modelled as [35]:

$$P_{out}(t) = P_{in}(t)e^{G(t)} \tag{8}$$

$$\phi_{out}(t) = \phi_{in}(t) - \frac{1}{2}\alpha_A G(t) \tag{9}$$

$$\frac{dG(t)}{dt} = \frac{G_0 - G(t)}{\tau_c} - \frac{P_{in}(t)}{E_{sat}}\left[e^{G(t)} - 1\right] \tag{10}$$

where $P_{in}(t)$ and $\phi_{in}(t)$ are the power and the phase of the input optical field, respectively, $P_{out}(t)$ and $\phi_{out}(t)$ are the power and the phase of the output optical field, respectively, $G(t)$ represents the integrated gain at each point of the pulse profile, e^{G0} is the unsaturated single-pass gain of the amplifier, α_A is the line width enhancement factor, τ_c is the spontaneous carrier lifetime, and E_{sat} is the saturation energy. The following model parameters have been used in the simulations: $\tau_c = 100$ ps, $\alpha_A = 5$, and $E_{sat} = 5$ pJ.

The standard single-mode fibre (SMF) was modelled using the low-pass transfer function with first order dispersion of 17 ps/(nm km). The PIN photodiode, the receiver main amplifier (AMP), and the low-pass filter (LPF) have been jointly modelled as a low-pass RC filter with the 3-dB bandwidth required by the DST method.

For performance evaluation, a pure semianalytical method has been used, which combines noiseless signal transmission simulation with noise analysis in optical transmission systems using directly modulated MQW lasers and optically preamplified direct-detection receivers. Using that method with the Gaussian approximation, the average error probability has been estimated as in [36]. The optical amplifier noise model we use here is based on the model originally derived for semiconductor optical amplifiers [37], and further extended to fibre amplifiers [38, 39]. In our model, the signal photocurrent I_k is obtained by simulation, and signal dependent noise terms are evaluated for each bit of the PRBS. The voltage due to laser noise after the receiver filter is also included since it is responsible for the BER floor at 10 Gbit/s for distances around 253 km in the DST system [31]. The standard deviation of the noise voltage for the k-th bit of the PRBS is given by:

$$\sigma_k^2 = \sigma_{s-sp}^2 + \sigma_{sp-sp}^2 + \sigma_{sh}^2 + \sigma_{th}^2 + \sigma_{ld}^2 \qquad (11)$$

where σ_{s-sp}^2 is the variance of the signal-ASE beat noise voltage, σ_{sp-sp}^2 is the variance of the ASE–ASE beat noise voltage, σ_{sh}^2 is the variance of the shot noise voltage, and σ_{th}^2 is the variance of the thermal noise voltage, and σ_{ld}^2 is the voltage due to the laser noise after the receiver filter. I_{sp} being the spontaneous emission noise photocurrent given by [39]:

$$I_{sp} = 2\frac{\eta q}{h\nu} n_{sp}(G-1)h\nu B_o L_a \qquad (12)$$

variances of the noise voltage terms are given by:

$$\sigma_{s-sp}^2 = 2Z_R^2 I_k I_{sp}\frac{B_e}{B_o} \qquad (13)$$

$$\sigma_{sp-sp}^2 = Z_R^2 I_{sp}^2 \frac{B_e}{B_o}\left(1 - \frac{B_e}{2B_o}\right) \qquad (14)$$

$$\sigma_{sh}^2 = 2B_e q Z_R^2 [I_k + I_{sp}] \qquad (15)$$

$$\sigma_{th}^2 = Z_R^2 I_{th}^2 B_e \qquad (16)$$

$$\sigma_{ld}^2 = I_k^2 Z_R^2 \int_0^{\infty} S_{out}(\omega)|H_R(\omega)|^2 d\omega \qquad (17)$$

where B_e is the electrical bandwidth, B_o is the optical bandwidth, η is the quantum efficiency of the PIN photodiode, q is the electronic charge, h is Plank's constant, ν is the optical frequency, G is the optical preamplifier gain, L_a is the loss between the optical preamplifier output and the photodetector input, n_{sp} is the spontaneous emission factor of the EDFA, Z_R is the receiver transimpedance, I_{th} is the spectral current density of the thermal noise, which is assumed to be 10 pA/$\sqrt{}$Hz, $H_R(\omega)$ is the receiver transfer function, and $S_{out}(\omega)$ is the power spectral density of the laser intensity noise at the fibre output given in [40].

4 Simulation results and discussion

Using the simulation methodology described in Section 3 with the laser parameters proposed in Section 2, we assess, in this Section, the performance of DST systems operated at 20 Gbit/s. For each fibre length, the system parameters, namely the laser bias current, the modulation current, and the receiver cut-off frequency, have been adjusted in order to minimise the input mean optical power of the EDFA preamplifier for an average error probability (BER) of 10^{-9} (receiver sensitivity). Since, in practical systems, a limit for the maximum laser peak current is imposed in order to avoid the damage of the laser, in this work the maximum laser peak current was limited to 90 mA.

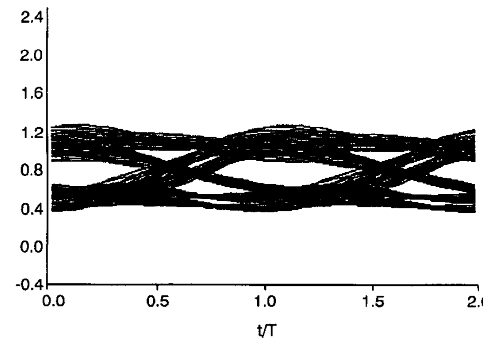

Fig. 3 *Eye diagram at output of receiver low-pass filter after 50 km of SMF using EDFA as booster amplifier*

Fig. 3 shows the eye diagram after DST over 50 km of SMF, assuming that the EDFA is used as a booster amplifier. This eye diagram is similar to those obtained in binary DST experiments reported by Wedding *et al.* [32]. Figs. 4 and 5 show eye diagrams for DST over 50 km using a SOA with unsaturated gains of 20 and 25 dB, respectively. The corresponding average error probabilities (BER) are shown in Fig. 6. As can be seen in this Figure, the performance degradation after DST over 50 km of SMF, due to the use of a SOA, is 2.5 and 4.9 dB for unsaturated gains of 20 and 25 dB, respectively.

Fig. 7 shows the receiver sensitivity vs. fibre length for DST at 20 Gbit/s, assuming that an EDFA or a SOA is used as a booster amplifier. As may be seen, the system performance is improved due to the use of a SOA with an unsaturated gain of 20 dB, for link lengths ranging from 8 to 20 km. In this region, the laser chirp reduction in the

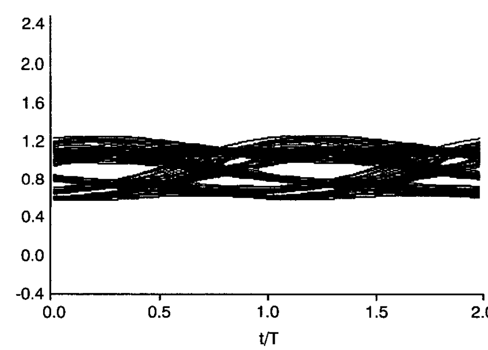

Fig. 4 *Eye diagram at output of receiver low-pass filter after 50 km of SMF using SOA with unsaturated gain of 20 dB as booster amplifier*

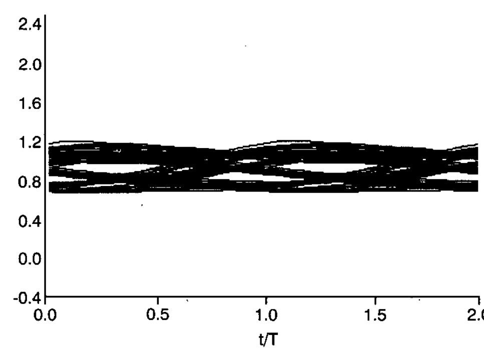

Fig. 5 *Eye diagram at output of receiver low-pass filter after 50 km of SMF using SOA with unsaturated gain of 25 dB as booster amplifier*

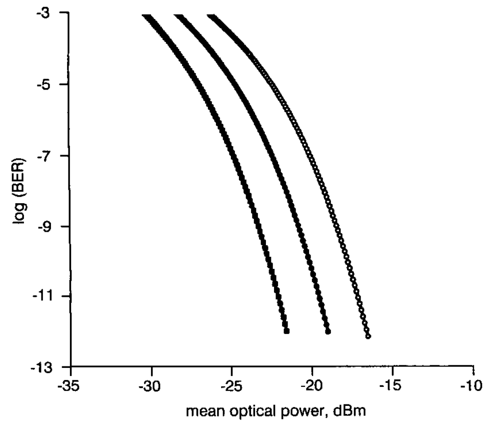

Fig. 6 *Average error probability (BER) at 20 Gbit/s after DST over 50 km of SMF using EDFA or SOA as booster amplifier*
—■— EDFA
—●— SOA (20 dB)
—○— SOA (25 dB)

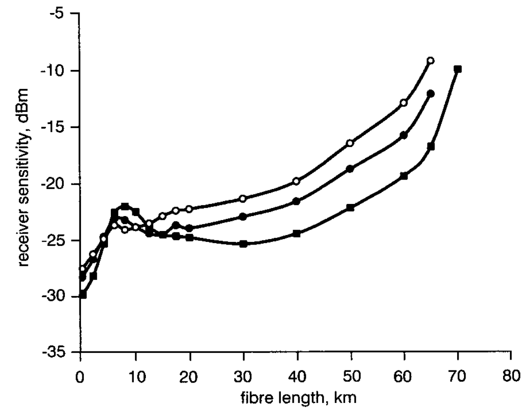

Fig. 8 *Receiver sensitivity for DST at 20 Gbit/s against fibre length assuming that laser line width enhancement factor (α) is equal to 3*
—■— DST (EDFA)
—●— DST (SOA, 20 dB)
—○— DST (SOA, 25 dB)

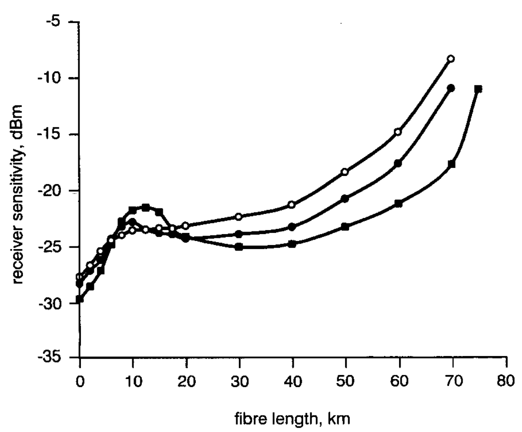

Fig. 7 *Receiver sensitivity for DST at 20 Gbit/s aganist fibre length assuming that EDFA or SOA is used as booster amplifier*
—■— DST (EDFA)
—●— DST (SOA, 20 dB)
—○— DST (SOA, 25 dB)

SOA reduces dispersion penalties induced by chirp and fibre dispersion interaction. For link lengths larger than 20 km, gain saturation effects in the SOA dominate over the influence of chirp reduction and, as a consequence, sensitivity degradation is observed. For link lengths ranging from 30 to 50 km, the sensitivity reduction ranges between 1.2 dB at 30 km and 2.5 dB at 50 km, due to the use of the SOA instead of the EDFA. The increase of the unsaturated SOA gain from 20 to 25 dB is only advantageous for link lengths ranging from 8 to about 12.5 km, where a small performance improvement less than or equal to 0.8 dB is observed.

In Fig. 8, we have increased the laser line width enhancement factor (α) to 3, in order to investigate the influence of this parameter on the receiver sensitivity of DST systems at 20 Gbit/s. As may be seen, the system performance is improved due to the use of a SOA with an unsaturated gain of 20 dB, for link lengths ranging from 6 to 12.5 km. For link lengths ranging from 30 to 50 km, the sensitivity reduction ranges between 2.5 dB at 30 km and 3.5 dB at 50 km, due to the use of the SOA instead of the EDFA. For this value of the line width enhancement factor, the increase of the unsaturated SOA gain from 20 to 25 dB is only advantageous for link lengths ranging from 4 to 10 km, where a small performance improvement less than or equal to 0.85 dB is observed.

5 Conclusions

We have proposed a set of MQW laser parameters suitable for simulation of optical transmission systems at 20 Gbit/s. The parameters have been estimated by joint fitting of an IM response model to five measured IM response curves of a strained layer MQW laser. Using this set of laser parameters, we have assessed the performance of 20 Gbit/s dispersion supported transmission systems incorporating an EDFA or a SOA as a booster amplifier. The proposed laser parameters may also be used for simulation of 40 Gbit/s four-level DST systems, since they require only half the bandwidth of a 40 Gbit/s binary system.

6 Acknowledgments

This work has been supported by the Institute of Telecommunications at Coimbra, Portugal.

7 References

1 MOHRDIEK, S., BURKHARD, H., STEINHAGEN, F., HILLMER, H., LÖSCH, R., SCHLAPP, W., and GÖBEL, R.: '10-Gb/s standard fiber transmission using directly modulated 1.55-μm quantum well DFB lasers', *IEEE Photonics Technol. Lett.*, 1995, **7**, (11), pp. 1357–1359

2 CARTLEDGE, J., and SRINIVASAN, R.: 'Extraction of DFB laser rate equation parameters for system simulation purposes', *IEEE/OSA J. Lightwave Technol.*, 1997, **15**, (5), 852–860

3 SALGADO, H., FERREIRA, J.M., and O'REILLY, J.J.: 'Extraction of semiconductor intrinsic laser parameters by intermodulation distortion analysis', *IEEE Photonics Technol. Lett.*, 1997, **9**, (10), pp. 1331–1333

4 WEDDING, B., PÖHLMANN, W., and FRANZ, B., GEUPEL, H.: 'Multi-level dispersion supported transmission at 20 Gbit/s over 46 km installed standard singlemode fibre', 22nd European conference on *Optical Communications*, ECOC'96, 1996, Oslo, Norway, pp. 1.91–1.94

5 WEDDING, B., IDLER, W., FRANZ, B., PÖHLMANN, W., and LACH, E.: '40 Gbit/s quaternary dispersion supported transmission over 31 km standard singlemode fibre without optical dispersion compensation', 24th European conference on *Optical Communications*, ECOC'98, 1998, Madrid, Spain, pp. 523–524

6 MEDEIROS, C.R., and O'REILLY, J.J.: 'Chirp compensation capability of a semiconductor laser amplifier', *Electron. Lett.*, 1991, **27**, (8), pp 649–650

7 DALL'ARA, R.: 'SOA applications: technical requirements and market overview', COST240 workshop: SOA-based components for optical networks, 1997, Prague, The Czech Republic, pp. 8.1–8.2

8 URL: http://www.intec.rug.ac.be/Research/Projects/COST240/exercise 10.html

9 GUEKOS, G.: 'Photonic devices for telecommunications' (Springer-Verlag, 1999)

10 GUEKOS, G.: FAULKNER, D.W. and HARMER, A.L. (Eds.): 'Research on optical communications in Europe the Programme COST', in 'Broadband superhighway, networks and optical communications (NOC'96)' (IOS Press, Amsterdam, 1996), **1**, pp. 15–21

11 NAGARAJAN, R., ISHIKAWA, M., FUKUSHIMA, T., GEELS, R., and BOWERS, J.: 'High speed quantum well lasers and carrier transport effects', *IEEE J. Quantum Electron.*, 1992, **28**, (10), pp. 1990–2008

12 ISHIKAWA, M., NAGARAJAN, R., FUKUSHIMA, T., WASSERBAUER, J.G., and BOWERS, J. E.: 'Long wavelength high-speed semiconductor lasers with carrier transport effects', *IEEE J. Quantum Electron.*, 1992, **28**, (10), pp. 2230–2241

13 AGRAWAL, G., and DUTTA, N.: 'Long-wavelength semiconductor lasers' (Van Nostrand Reinhold Company, New York, 1986),

14 ACKERMAN, D.A., SHTENGEL, G.E., HYBERTSEN, M.S., MORTON, P.A., KAZARINOV, R.F., TANBUN-EK, T., and LOGAN, R.A.: 'Analysis of gain in determining T_0 in 1.3 μm semiconductor lasers', *IEEE J. Sel. Topics in Quantum Electron.*, 1995, **1**, (2), pp. 250–263

15 DUTTA, N.K., and NELSON, R.J.: 'The case of Auger recombination in $In_{1-x}Ga_xAs_yP_{1-y}$', *J. Appl. Phys.*, 1982, **53**, (1), pp. 74–92

16 WANG, M.C., KASH, K., ZAH, C.E., BHAT, R., and CHUANG, S.L.: 'Measurement of nonradiative and radiative recombination rates in strained-layer quantum well systems', *Appl. Phys. Lett.*, 1993, **62**, pp. 166–168

17 THIJS, P.J.A., TIEMEIJER, L.F., BINSMA, J.J.M., and VAN DONGEN, T.: 'Progress in long-wavelength strained-layer InGaAs(P) quantum well semiconductor lasers and amplifiers', *IEEE J. Quantum Electron.*, 1994, **30**, (2), pp. 477–499

18 O'REILLY, E.P., and SILVER, M.: 'Temperature sensitivity and high temperature operation of long wavelength semiconductor lasers', *Appl. Phys. Lett.*, 1993, **63**, (24), pp. 3318–3320

19 SWEENEY, S.J., PHILIPS, A.F., ADAMS, A.R., O'REILLY, E.P., and THIJS, P.J.A.: 'The effect of temperature dependent processes on the performance of 1.5-μm compressively strained InGaAs(P) MQW semiconductor diode lasers', *IEEE Photonics Technol. Lett.*, 1998, **10**, (8), pp. 1076–1078

20 ADAMS, A.R., ASADA, M., SUEMATSU, Y., and ARAI, S.: 'The temperature dependence of the efficiency and threshold current of $In_{1-x}Ga_xAS_yP_{1-y}$ lasers related to intervalence band absorption', *Jpn. J. Appl. Phys.*, 1980, **19**, (10), pp. 621–624

21 ASADA, M., and SUEMATSU, Y.: 'The effect of loss and nonradiative recombination on the temperature dependence of threshold current in 1.5–1.6 μm GaInAsP/InP lasers', *IEEE J. Quantum Electron.*, 1983, **QE-19**, (6), pp. 917–923

22 ZOU, Y., OSINSKI, J.S., GRODZINSKI, P., DAPKUS, P.D., RIDEOUT, W.C., SHARFIN, W.F., SCHLAFER, J., and CRAWFORD, F.D.: 'Experimental study of Auger recombination, gain, and temperature sensitivity of 1.5μm compressively strained semiconductor lasers', *IEEE J. Quantum Electron.*, 1993, **29**, (6), pp. 1565–1575

23 O'GORMAN, J., LEVI, A.F.J., SCHMITT-RINK, S., TANBUN-EK, T., COBLENTZ, D.L., and LOGAN, R.A.: 'On the temperature sensitivity of semiconductor lasers', *Appl. Phys. Lett.*, 1992, **60**, (2), pp. 157–159

24 PANKOVE, J.I.: 'Temperature dependence of emission efficiency and lasing threshold in laser diodes', *IEEE J. Quantum Electron.*, 1968, **QE-4**, (4), pp. 119–122

25 EVANS, J.D., and SIMMONS, J.G.: 'New insight into the temperature sensitivity of the threshold current of long wavelength semiconductor lasers', 14th international *Semiconductor Laser* conference, 1994, Maui, Hawaii, USA, pp. 237–238

26 BYRNE, D.M., and KEATING, B.A.: 'A laser model based on temperature dependent rate equations', *IEEE Photonics Technol. Lett.*, 1989, **1**, (11), pp. 356–359

27 FREIRE, M.M., and DA SILVA, H.J.A.: 'Performance assessment of high density wavelength division multiplexing systems with dispersion supported transmission at 10 Gbit/s', Second IEEE symposium on *Computers and Communications*, ISCC'97, 1997, Alexandria, Egypt, pp. 318–322

28 RIBEIRO, R.F., DA ROCHA, J.F., CARTAXO, A.V.T., DA SILVA, H.J. A., FRANZ, B., and WEDDING, B.: 'FM response of quantum well lasers taking into account carrier transport effects', *IEEE Photonics Technol. Lett.*, 1995, **7**, (8), pp. 857–859

29 PRESS, W., FLANNERY, B., TEUKOLSKY, S., and VETTERLING, W.: 'Numerical recipes' (Cambridge University Press, Cambridge, 1986)

30 CHO, S., LU, C., HOVINEN, M., AM, VUSIRIKALA, V., SONG, J., JOHNSON, F., STONE, D., and DAGENAIS, M.: 'Dependence of the linewidth enhancement factor on the number of compressively strained quantum well in lasers', *IEEE Photonics Technol. Lett.*, 1997, **9**, (8), pp. 1081–1083

31 RIBEIRO, R.F.S., DA ROCHA, J.R.F., and CARTAXO, A.V.T.: 'Influence of laser phase noise on dispersive optical fiber communication systems', *IEEE Photonics Technol. Lett.*, 1995, **7**, (12), pp. 1510–1512

32 WEDDING, B., FRANZ, B., and JUNGINGER, B.: '10-Gb/s optical transmission up to 253 km via standard single-mode fiber using the method of dispersion-supported transmission', *IEEE/OSA J. Lightwave Technol.*, 1994, **12**, (10), pp. 1720–1727

33 FREIRE, M.M., and DA SILVA, H.J.A., FAULKNER, D.W. and HARMER, A.L. (Eds.): 'Performance improvement of 10-Gb/s four-channel WDM dispersion-supported transmission by using multi-layer thin film interference filters as demultiplexers', in Photonic networks, optical technology and infrastructure, networks and optical communications (NOC'97) (IOS Press, Amsterdam, 1997), **III**, pp. 135–140

34 FREIRE, M.M., and DA SILVA, H.J.A.: 'Performance improvement of 40-Gb/s capacity four-channel WDM dispersion-supported transmission by using broadened passband arrayed-waveguide grating demultiplexers', The Pacific Rim conference on *Lasers and Electro-optics*, CLEO/Pacific Rim'97, 1997, Chiba, Japan, pp. 13–14

35 AGRAWAL, G.P., and OLSSON, N.A.: 'Self phase modulation and spectral broadening of optical pulses in semiconductor laser amplifiers', *IEEE J. Quantum Electron.*, 1989, **25**, (11), pp. 2297–2306

36 FREIRE, M.M., and DA SILVA, H.J.A.: 'Performance assessment of two-channel dispersion-supported transmission systems using single- and double-cavity Fabry–Perot filters as demultiplexers', *IEEE Photonics Technol. Lett.*, 1995, **7**, (11), pp. 1360–1362

37 OLSSON, N. A.: 'Lightwave systems with optical amplifiers', *IEEE/OSA J. Lightwave Technol.*, 1989, **7**, (7), pp. 1071–1082

38 INOUE, K., TOBA, H., and NOSU, K.: 'Multichannel amplification utilizing an Er^{3+}-doped fiber amplifier', *IEEE/OSA J. Lightwave Technol.*, 1991, **9**, (3), pp. 368–374

39 PARK, Y.K., and GRANLUND, S.W.: 'Optical preamplifier receivers: application to long-hall digital transmission', *Optical Fiber Technol.*, 1994, **1**, pp. 59–71

40 WANG, J., PETERMANN, K.: 'Small signal analysis for dispersive optical fiber communication systems', *IEEE/OSA J. Lightwave Technol.*, 1992, **10**, (1), pp. 96–100